Metal-metal bonding in pentamethylcyclopentadienylmolybdenum(IV) dinuclear compounds: chloride abstraction from non-bonded Cp⋆2Mo2Cl6 to afford bonded [Cp⋆2Mo2Cl5]+

Fatima Abugideiri, James Fettinger, Rinaldo Poli

Metal–metal bonding in pentamethylcyclopentadienylmolybdenum(IV) dinuclear compounds: chloride abstraction from non-bonded $Cp^*_2Mo_2Cl_6$ to afford bonded $[Cp^*_2Mo_2Cl_5]^+$ ☆

Fatima Abugideiri, James C. Fettinger, Rinaldo Poli*

Department of Chemistry and Biochemistry, University of Maryland, College Park, MD 20742, USA

Received 18 August 1994

Abstract

Chloride abstraction from $Cp^*_2Mo_2Cl_6$ ($Cp^* = \eta^5$-C_5Me_5) is accomplished by interaction with the Lewis acid $AlCl_3$ to afford the structurally characterized salt $[Cp^*_2Mo_2Cl_5]^+[AlCl_4]^-$. Crystal data: triclinic, space group $P\bar{1}$, $a = 8.3903(13)$, $b = 15.797(3)$, $c = 24.036(2)$ Å, $\alpha = 86.766(11)$, $\beta = 80.916(10)$, $\gamma = 81.616(14)°$, $V = 3110.5(8)$ Å^3, $D_c = 1.726$ Mg m^{-3}, μ(Mo Kα) = 1.618 mm^{-1}, $R = 0.0637$. The structure exhibits two four-legged piano stools joined by three bridging Cl atoms. The Mo–Mo distance of 2.866(2) Å is significantly longer than all other reported bonded Mo(IV)–Mo(IV) distances and longer than the single bond ($\sigma^2\delta^{*2}\delta^2$) distance in the related Mo(III) complexes $[(ring)MoCl_2]_2$ (ring = substitute cyclopentadienyl ring). The reasons for this lengthening are analyzed and discussed on the basis of structural data and Fenske–Hall MO calculations. $[Cp^*_2Mo_2Cl_5]^+$ reacts rapidly with Cl^- to afford $[Cp^*MoCl_4]^-$ and exhibits a reversible one-electron oxidation to a neutral $Cp^*_2Mo_2Cl_5$ species at −0.13 V versus ferrocene/ferricinium. The non-existence of a metal–metal bonded isomeric form of the $Cp^*_2Mo_2Cl_6$ parent compound is also discussed.

Keywords: Crystal structures; Metal–metal bonding; Molybdenum complexes; Pentamethylcyclopentadienyl complexes; Dinuclear complexes

1. Introduction

The general question of whether two metals held together in a dinuclear compound by bridging ligands are also able to establish a direct bonding interaction has attracted considerable attention [1]. For complexes of 4d and 5d elements, the formation of a bond is the rule, but there are nevertheless a considerable number of exceptions. For instance, whereas edge-sharing bioctahedral $Re_2Cl_4(\mu\text{-}Cl)_2(\mu\text{-}dppm)_2$ exhibits a metal–metal bond [2], the metals are non-bonded in the similar $Re_2Cl_4(\mu\text{-}Cl)_2(dppe)_2$ compound [3] (dppm = bid(diphenylphosphino)methane; dppe = bis(diphenylphosphino)ethane) and the two Ru(III) compounds $Ru_2Cl_4(\mu\text{-}Cl)_2(\mu\text{-}dmpm)_2$ and $Ru_2Cl_4(\mu\text{-}Cl)_2(PBu_3)_4$ (dmpm = bis(dimethylphosphino)methane) are analogously bonded and non-bonded, respectively [2,4]. An even more striking situation is found in the pair of $Mo_2Cl_4(\mu\text{-}Cl)_2L_4$ (L = PMe_2Ph, PEt_3) complexes having not only an identical coordination geometry but also identical stereochemistry, where a metal–metal bond exists in the former but not in the latter [5]. The strength of the metal–metal interaction increases steadily along the series of $Mo_2Cl_4(\mu\text{-}Cl)_2(PMe_xEt_{3-x})_4$ complexes ($x = 0, 1, 2, 3$) [6]. A metal–metal bond is also *not* formed in the dinuclear M_2Cl_{10} compounds (M = W, d^1–d^1 or Re, d^2–d^2), whereas this is present in the corresponding $M_2(OMe)_{10}$ compounds [7]. For cyclopentadienyl-substituted complexes, two different forms of $Cp^*_2Ru_2Cl_2(\mu\text{-}Cl)_2$ co-crystallize in a 1:1 ratio, only one of them having an Ru–Ru bond, the geometry of the two forms being otherwise identical [8].

This contribution deals with Cp*–Mo(IV) systems. Compound $Cp^*_2Mo_2Cl_6$, recently reported by us [9], was found to have structure **I** with no metal–metal bond between the two d^2 Mo(IV) centers. This geometry is identical to that observed for the d^1 Ta(IV) complex $(C_5Me_4Et)_2Ta_2Br_6$ (also lacking a metal–metal inter-

☆ Dedicated to Professor F.A. Cotton on the occasion of his 65th birthday.

*Corresponding author.

action) [10], whereas the d^3 Re(IV) compound $(C_5Me_4Et)_2Re_2Cl_6$ exists in the alternative, metal–metal bonded structure **II** [11]. We will show here that the metal–metal non-bonded $Cp^*_2Mo_2Cl_6$ molecule rearranges to a metal–metal bonded structure upon abstraction of a Cl^- ligand. We also report a theoretical investigation of the $[Cp^*_2Mo_2Cl_5]^+$ ion and discuss the possible reasons for the weakening of the Mo–Mo bond interaction along the series of Mo(IV) compounds $[Cp^*_2Mo_2Cl_4]^{2+}$, $[Cp^*_2Mo_2Cl_5]^+$ and $Cp^*_2Mo_2Cl_6$.

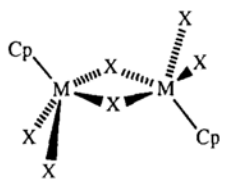

I

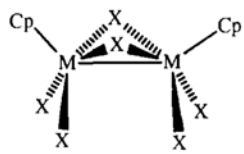

II

2. Experimental

2.1. General

All operations were carried out under an atmosphere of dinitrogen with standard Schlenk-line and glove-box techniques. Solvents were purified by conventional methods and distilled under dinitrogen prior to use. NMR spectra were obtained with a Bruker AF200 spectrometer; the peak positions are reported upfield of TMS as calculated form the residual solvent peaks. Cyclic voltammograms were recorded with an EG&G 362 potentiostat connected to a Macintosh computer through MacLab hardware/software; the electrochemical cell was a locally modified Schlenk tube with a Pt counter electrode sealed through uranium glass/Pyrex glass seals. The cell was fitted with an Ag/AgCl reference electrode and a Pt working electrode. Measurements were carried out with n-Bu_4NPF_6 (~0.1 M) as the supporting electrolyte and potentials are reported versus the Cp_2Fe/Cp_2Fe^+ couple which was introduced into the cell at the end of each measurement. $Cp^*_2Mo_2Cl_6$ was prepared as previously described [9]. $AlCl_3$ (Aldrich) was sublimed prior to use and $[Ph_3PNPPh_3]^+Cl^-$ (Aldrich) was used as received.

2.2. Preparation of $[Cp^*_2Mo_2Cl_5][AlCl_4]$

$Cp^*_2Mo_2Cl_6$ (310 mg, 0.46 mmol) and $AlCl_3$ (122 mg, 0.915 mmol) were introduced in a Schlenk tube equipped with a magnetic stirrer bar. Dichloromethane (30 ml) was added and the resulting mixture was stirred at room temperature. The formation of an orange–brown solution and a small amount of a pale green precipitate was observed. Stirring was continued overnight with no further change, after which time the mixture was filtered and the mother liquor was layered with heptane (70 ml). Diffusion of the layers at room temperature produced more powdery green precipitate, a small amount of red microcrystals, and well-formed black crystals. The green powder was eliminated by repeatedly washing with heptane and decanting off the turbid green liquid from the heavier crystalline precipitate until clear washings were obtained. The mixture of crystals (the greater portion of them being the larger black ones) were dried under vacuum. Yield 107 mg (28%). A black crystal from this crop was identified as $[Cp^*_2Mo_2Cl_5][AlCl_4]$ by X-ray crystallography (vide infra). ^1H NMR (CD_2Cl_2, room temperature, δ): 2.36 (s), 1.35 (br s, $w_{1/2}=25$ Hz), −4.2 (br s, $w_{1/2}=50$ Hz) (relative integrate intensity: 11:4.6:1). The strongest and sharp resonance at δ 2.39 is therefore assigned to $[Cp^*_2Mo_2Cl_5][AlCl_4]$, whereas the broad resonance at δ 1.35 is due to $Cp^*_2Mo_2Cl_5$ and that at δ −4.2 is due to $Cp^*_2Mo_2Cl_6$, following assignments previously made [9]. The $Cp^*_2Mo_2Cl_6$ material probably forms from $[Cp^*_2Mo_2Cl_5][AlCl_4]$ by solution equilibria (see Section 3). Consequently, the red microcrystals probably consist of $Cp^*_2Mo_2Cl_5$ but further studies aimed at characterizing this material were not carried out. This assignment is also consistent with the results of the cyclic voltammetric experiment (see Section 3).

The reaction between $[Cp^*_2Mo_2Cl_5][AlCl_4]$ and Cl^- was carried out in an NMR tube. To a CD_2Cl_2 solution of the above crystals (7 mg) was added an excess of $[Ph_3PNPPh_3]^+Cl^-$ (~15 mg); the color of the solution changed immediately from orange to yellow. The ^1H NMR at room temperature showed a broad resonance at δ −14.0 ($w_{1/2}=150$ Hz), which corresponds to $[Cp^*MoCl_4]^-$ [9], as the only Cp* resonance.

2.3. X-ray crystallography

A black crystal with approximate dimensions $0.60\times0.25\times0.25$ mm in a parallelepiped habit was glued on the inside of a thin-walled glass capillary which was then flame-sealed under dinitrogen and placed on the Enraf-Nonius CAD-4 diffractometer. The cell parameters and orientation matrix were determined from 25 reflections in the range $16.1<\theta<24.4°$ and confirmed with axial photographs. Three nearly orthogonal standard reflections were monitored at 1 h intervals of X-ray exposure showing no significant variations in intensity. An absorption correction [12a] based on four ψ-scan reflections over the θ range 7.3–9.2°, each collected twice, was applied (transmission factors varied from 0.752 to 0.998 with an average of 0.900). Data corrections for Lorentz and polarization factors, absorption, and data reduction to observed structure-factor amplitudes were carried out using the program package NRCVax [12b].

The structure was developed in the centrosymmetric triclinic space group $P\bar{1}$, which was confirmed by the successful refinement of the structure. All heavy atoms (Mo, Cl, Al) were located by direct methods with the program SHELXS [12c], further indicating that the asymmetric unit is composed of four fragments, two anions and two cations. The carbon atoms were located and refined by successive full-matrix least-squares cycles and difference-Fourier maps. Several cycles of refinement, first isotropically and then anisotropically, converged smoothly and revealed possible rotational disorder in the Cp* ligand attached to Mo(2). This was evidenced by the large thermal parameters directed in the direction of libration. Further refinement, implementing idealization commands (AFIX) in SHELXL, allowed for the isotropic refinement of two Cp* rings rotationally offset by 19.1°. These partial occupancy moieties had their thermal parameters constrained to be the same for all atoms allowing for occupancy refinement that converged to 0.524:0.476. At this point the occupancy was fixed and the thermal parameter of each individual partial occupancy carbon atom was freely refined isotropically. Methyl hydrogen atoms were placed in calculated positions and forced to ride on the parent carbon atom during the refinement with U_H set equal to $1.5U$ of the attached C atom. The highest peak in the final difference-Fourier map (>1 e Å^{-3}) are within 0.1 Å from the heavy atoms. Selected crystal data are collected in Table 1, fractional atomic coordinates are in Table 2 and selected bond distances and angles are listed in Table 3. All crystallographic calculations were performed on a Personal computer (PC) with a 486 DX2/66 processor and 16Mb of extended memory.

Table 1
Crystal data and structure refinement for $[Cp^*_2Mo_2Cl_5][AlCl_4]$

Empirical formula	$C_{20}H_{30}AlCl_9Mo_2$
Formula weight	808.35
Temperature (K)	293(2)
Wavelength (Å)	0.71069
Crystal system	triclinic
Space group	$P\bar{1}$
Unit cell dimensions	
a (Å)	8.3903(13)
b (Å)	15.797(3)
c (Å)	24.036(2)
α (°)	86.766(11)
β (°)	80.916(10)
γ	81.616(14)
Volume (Å^3)	3110.5(8)
Z	4
Density (calc.) (Mg m^{-3})	1.726
Absorption coefficient (mm^{-1})	1.618
F(000)	1600
Crystal size (mm)	0.60×0.25×0.25
θ Range for data collection (°)	1.54–19.98
Index ranges	$-7 \leqslant h \leqslant 8$, $0 \leqslant k \leqslant 15$, $-22 \leqslant l \leqslant 23$
Reflections collected	5840
Independent reflections	5775
Refinement method	full-matrix least-squares on F^2
Observed data ($I > 2\sigma(I)$)	3614
Restraints/parameters	0/528
Goodness of fit on F^2	1.034
Final R indices	
$R1$	0.0637
w$R2$	0.1449
R indices (all data)	
$R1$	0.1159
$wR2$	0.1701
Largest difference peak and hole (e Å^{-3})	1.275 and −0.691

2.4. MO calculations

The Fenske–Hall MO treatment [13] was carried out on the model compound $[Cp_2Mo_2Cl_5]^+$. A minimum basis set was employed and the atomic 1s, 2s, 2p, 3s, 3p, 3d, 4s and 4p orbitals of the Mo atoms, the 1s, 2s and 2p orbitals of the Cl atoms, and the 1s orbital of the C atoms were treated as 'core'. Atomic parameters for the $[Cp^*_2Mo_2Cl_5]^+$ ions (two crystallographically independent fragments) were averaged in order to idealize the geometry to C_{2v} symmetry. The Cp* ligands were replaced by Cp ligands, which were placed in such a way that the unique carbon atom (sitting on the mirror plane) is eclipsed with the terminal Mo–Cl bond, and the Cp hydrogen atoms were placed in the ring plane radially at a distance of 0.95 Å from the corresponding C atoms. A high-handed coordinate system was chosen, with the z axis parallel to the Mo–Mo vector and the xz plane parallel to the plane identified by the two MO atoms and the unique (axial) bridging Cl atom. The local coordinate system chosen for the two Mo atoms has the z axis along the corresponding Mo–CNT vector and the y axis in the plane containing the two Mo atoms, the terminal Cl atoms, and the axial bridging atom; the local coordinate systems for all the Cl atoms coincide with the master coordinate system.

3. Results and discussion

3.1. Synthesis

We recently reported the formation of $Cp^*_2Mo_2Cl_6$ by conproportionation of $Cp^*_2Mo_2Cl_4$ and Cp^*MoCl_4 and proposed, on the basis of combined ^{1}H NMR monitoring and electrochemical studies, that the last step of this process is a chloride transfer from the anion to the cation in the (unobserved) $[Cp^*_2Mo_2Cl_5]^+[Cp^*MoCl_4]^-$ intermediate (Eq. (1) [9]. In order to obtain supporting evidence for the likelihood of the $[Cp^*_2Mo_2Cl_5]^+$ ion as an intermediate, we have

Table 2
Atomic coordinates ($\times 10^4$) and equivalent isotropic displacement parameters ($Å^2 \times 10^3$) for $[Cp^*_2Mo_2Cl_5][AlCl_4]$

	x	y	z	U_{eq} [a]
Mo(1)	983(2)	1885(1)	4434(1)	46(1)
Mo(2)	1362(2)	2607(1)	5464(1)	47(1)
Mo(3)	−421(2)	3146(1)	9463(1)	48(1)
Mo(4)	−2024(2)	2399(1)	10478(1)	47(1)
Cl(10)	−1349(6)	1258(3)	4822(2)	87(2)
Cl(20)	−882(6)	2064(3)	5991(2)	83(2)
Cl(30)	1326(6)	3796(3)	9938(2)	82(2)
Cl(40)	−437(7)	2958(3)	11062(2)	87(2)
Cl(11)	−497(5)	3222(3)	4819(2)	68(1)
Cl(12)	3081(5)	2753(3)	4555(2)	68(1)
Cl(13)	2349(6)	1144(3)	5179(2)	71(1)
Cl(31)	−2635(6)	2265(3)	9526(2)	76(2)
Cl(32)	−2682(6)	3854(3)	10116(2)	79(2)
Cl(33)	544(5)	1812(3)	9928(2)	60(1)
Al(1)	6308(7)	88(4)	7943(2)	69(2)
Cl(1)	7449(8)	−1189(4)	7824(3)	129(2)
Cl(2)	6089(8)	360(4)	8810(2)	102(2)
Cl(3)	3992(7)	190(4)	7691(3)	109(2)
Cl(4)	7696(11)	951(5)	7471(3)	172(4)
Al(2)	5749(7)	5109(4)	2964(2)	70(2)
Cl(5)	4544(8)	4546(4)	2402(2)	106(2)
Cl(6)	8318(8)	4858(5)	2732(3)	144(3)
Cl(7)	5098(8)	4604(5)	3785(2)	127(2)
Cl(8)	5042(9)	6432(4)	2911(3)	129(2)
C(10)	396(21)	1064(12)	3684(7)	56(5)
C(11)	2009(24)	868(10)	3754(6)	50(5)
C(12)	2794(19)	1611(13)	3620(7)	50(4)
C(13)	1600(28)	2267(13)	3484(6)	68(6)
C(14)	135(22)	1955(12)	3552(7)	60(5)
C(15)	−786(21)	424(12)	3693(8)	89(7)
C(16)	2866(25)	−7(12)	3872(7)	91(7)
C(17)	4573(23)	1645(16)	3548(8)	114(9)
C(18)	1835(27)	3172(11)	3295(8)	99(7)
C(19)	−1541(26)	2446(14)	3457(9)	114(8)
C(20) [b]	2219(16)	3870(9)	5720(6)	27(11)
C(21) [b]	1046(17)	3624(9)	6148(6)	66(12)
C(22) [b]	1703(17)	2867(9)	6398(6)	44(8)
C(23) [b]	3282(16)	2646(8)	6125(5)	45(8)
C(24) [b]	3601(15)	3265(8)	5705(5)	34(9)
C(25) [b]	2031(24)	4639(13)	5345(9)	78(11)
C(26) [b]	−608(25)	4086(13)	6309(9)	89(12)
C(27) [b]	869(25)	2384(13)	6872(8)	134(18)
C(28) [b]	4421(22)	1885(12)	6257(8)	63(10)
C(29) [b]	5138(21)	3278(12)	5313(8)	56(9)
C(20A) [c]	2442(16)	3799(9)	5652(6)	59(18)
C(21A) [c]	995(14)	3829(8)	6051(5)	20(8)
C(22A) [c]	1174(13)	3106(7)	6427(4)	22(7)
C(23A) [c]	2732(15)	2629(7)	6260(5)	48(10)
C(24A) [c]	3516(16)	3057(9)	5781(6)	62(13)
C(25A) [c]	2781(21)	4442(10)	5174(7)	65(11)
C(26A) [c]	−476(16)	4509(9)	6072(5)	75(12)
C(27A) [c]	−74(12)	2884(7)	6918(3)	84(13)
C(28A) [c]	3432(18)	1811(8)	6542(5)	85(13)
C(29A) [c]	5196(19)	2774(12)	5464(7)	106(16)
C(30)	−1031(9)	3339(5)	8555(2)	49(4)
C(31)	276(10)	2676(5)	8557(3)	49(4)
C(32)	1654(10)	3036(7)	8673(3)	49(4)
C(33)	1162(12)	3923(7)	8742(3)	58(5)
C(34)	−500(11)	4109(5)	8682(3)	48(4)
C(35)	−2604(10)	3298(8)	8379(3)	77(6)
C(36)	265(26)	1763(11)	8420(7)	87(7)
C(37)	3319(21)	2553(14)	8678(9)	106(8)
C(38)	2309(24)	4553(12)	8798(8)	93(7)
C(39)	−1475(24)	4978(11)	8681(8)	92(7)
C(40)	−4349(18)	1716(10)	10675(7)	44(4)
C(41)	−4415(21)	2285(10)	11103(8)	62(5)
C(42)	−3130(24)	1953(12)	11417(6)	57(5)
C(43)	−2163(18)	1266(11)	11110(7)	51(5)
C(44)	−3002(18)	1117(9)	10692(6)	42(4)
C(45)	−5698(20)	1738(11)	10328(7)	69(5)
C(46)	−5750(24)	2993(12)	11275(8)	100(7)
C(47)	−2891(26)	2253(14)	11972(7)	102(7)
C(48)	−718(23)	740(12)	11306(9)	93(7)
C(49)	−2475(22)	371(10)	10295(7)	73(6)

[a] U_{eq} is defined as one third of the trace of the orthogonalized U_{ij} tensor.
[b] Site occupancy factor = 0.524.
[c] Site occupancy factor = 0.476.

generated such an ion by interaction of $Cp^*_2Mo_2Cl_6$ with the strong Lewis acid $AlCl_3$ (Eq. (2)). A comparison of Eqs. (1) and (2) shows that $Cp^*_2Mo_2Cl_6$ is a poorer Lewis acid than $AlCl_3$ or, conversely, that $AlCl_4^-$ is a poorer Cl^- donor than $Cp^*MoCl_4^-$.

$$[Cp^*_2Mo_2Cl_5]^+[Cp^*MoCl_4]^- \longrightarrow \tfrac{3}{2}\, Cp^*_2Mo_2Cl_6 \qquad (1)$$

$$Cp^*_2Mo_2Cl_6 + AlCl_3 \longrightarrow [Cp^*_2Mo_2Cl_5]^+[AlCl_4]^- \qquad (2)$$

The product of Eq. (2) shows a single sharp ^1H NMR resonance at δ 2.36 in CD_2Cl_2, indicating that this compound is diamagnetic. This contrasts with the neutral parent compound, for which a broad and paramagnetically shifted resonance at δ −4.23 is observed in the same solvent at room temperature.

3.2. Molecular structure

The tetrachloroaluminate salt crystallizes from CH_2Cl_2/heptane in the form of black crystals in the triclinic space group $P\bar{1}$ with two independent cations and anions in the asymmetric unit. The tetrachloroaluminate ions show the expected regular tetrahedral geometry with an average Al–Cl length of 2.109(14) Å and Cl–Al–Cl angles in the narrow 107.4–111.7° range. Selected metric parameters of the two cations, which are geometrically equivalent, are shown side by side in Table 3 and one of the cations is shown in Fig. 1. Although there is no crystallographically imposed symmetry, the effective molecular symmetry of the cations is C_{2v}. The parameters are quite similar for the two independent cations and the small differences observed are probably the result of crystal packing effects. For the discussion of bond lengths and angles that follows,

Table 3
Selected bond distances (Å) and angles (°) for $[Cp^*_2Mo_2Cl_5][AlCl_4]$ [a]

Distances			
Mo(1)–Mo(2)	2.866(2)	Mo(3)–Mo(4)	2.874(2)
Mo(1)–Cl(10)	2.359(5)	Mo(3)–Cl(30)	2.366(5)
Mo(1)–Cl(11)	2.439(4)	Mo(3)–Cl(31)	2.461(4)
Mo(1)–Cl(12)	2.444(4)	Mo(3)–Cl(32)	2.440(5)
Mo(1)–Cl(13)	2.431(5)	Mo(3)–Cl(33)	2.423(4)
Mo(1)–CNT(1)	2.02(2)	Mo(3)–CNT(3)	2.009(7)
Mo(2)–Cl(11)	2.437(4)	Mo(4)–Cl(31)	2.451(4)
Mo(2)–Cl(12)	2.441(4)	Mo(4)–Cl(32)	2.431(5)
Mo(2)–Cl(13)	2.437(4)	Mo(4)–Cl(33)	2.430(5)
Mo(2)–Cl(20)	2.342(5)	Mo(4)–Cl(40)	2.366(5)
Mo(2)–CNT(2)	2.054(14)	Mo(4)–CNT(4)	2.008(14)
Angles			
Mo(2)–Mo(1)–Cl(10)	95.19(13)	Mo(4)–Mo(3)–Cl(30)	93.94(13)
Mo(2)–Mo(1)–Cl(11)	53.97(11)	Mo(4)–Mo(3)–Cl(31)	54.04(11)
Mo(2)–Mo(1)–Cl(12)	54.03(10)	Mo(4)–Mo(3)–Cl(32)	53.70(12)
Mo(2)–Mo(1)–Cl(13)	54.03(11)	Mo(4)–Mo(3)–Cl(33)	53.80(11)
Mo(2)–Mo(1)–CNT(1)	161.0(5)	Mo(4)–Mo(3)–CNT(3)	161.6(2)
Cl(10)–Mo(1)–Cl(11)	86.3(2)	Cl(30)–Mo(3)–Cl(31)	148.0(2)
Cl(10)–Mo(1)–Cl(12)	149.2(2)	Cl(30)–Mo(3)–Cl(32)	87.1(2)
Cl(10)–Mo(1)–Cl(13)	87.9(2)	Cl(30)–Mo(3)–Cl(33)	87.0(2)
Cl(10)–Mo(1)–CNT(1)	103.8(5)	Cl(30)–Mo(3)–CNT(3)	104.1(3)
Cl(11)–Mo(1)–Cl(12)	74.7(2)	Cl(31)–Mo(3)–Cl(32)	73.9(2)
Cl(11)–Mo(1)–Cl(13)	106.7(2)	Cl(31)–Mo(3)–Cl(33)	74.5(2)
Cl(11)–Mo(1)–CNT(1)	127.0(5)	Cl(31)–Mo(3)–CNT(3)	107.9(3)
Cl(12)–Mo(1)–Cl(13)	75.0(2)	Cl(32)–Mo(3)–Cl(33)	106.5(2)
Cl(12)–Mo(1)–CNT(1)	107.0(5)	Cl(32)–Mo(3)–CNT(3)	129.7(3)
Cl(13)–Mo(1)–CNT(1)	125.2(5)	Cl(33)–Mo(3)–CNT(3)	122.8(2)
Mo(1)–Mo(2)–Cl(11)	54.04(11)	Mo(3)–Mo(4)–Cl(31)	54.36(10)
Mo(1)–Mo(2)–Cl(12)	54.12(10)	Mo(3)–Mo(4)–Cl(32)	53.98(12)
Mo(1)–Mo(2)–Cl(13)	53.83(11)	Mo(3)–Mo(4)–Cl(33)	53.57(11)
Mo(1)–Mo(2)–Cl(20)	94.21(13)	Mo(3)–Mo(4)–Cl(40)	93.60(13)
Mo(1)–Mo(2)–CNT(2)	160.8(3)	Mo(3)–Mo(4)–CNT(4)	161.2(4)
Cl(11)–Mo(2)–Cl(12)	74.8(2)	Cl(31)–Mo(4)–Cl(32)	74.2(2)
Cl(11)–Mo(2)–Cl(13)	106.6(2)	Cl(31)–Mo(4)–Cl(33)	74.6(2)
Cl(11)–Mo(2)–Cl(20)	86.4(2)	Cl(31)–Mo(4)–Cl(40)	148.0(2)
Cl(11)–Mo(2)–CNT(2)	126.0(4)	Cl(31)–Mo(4)–CNT(4)	107.2(5)
Cl(12)–Mo(2)–Cl(20)	148.3(2)	Cl(32)–Mo(4)–Cl(40)	87.2(2)
Cl(12)–Mo(2)–Cl(13)	75.0(2)	Cl(32)–Mo(4)–Cl(33)	106.5(2)
Cl(12)–Mo(2)–CNT(2)	106.7(4)	Cl(32)–Mo(4)–CNT(4)	129.9(5)
Cl(13)–Mo(2)–Cl(20)	86.7(2)	Cl(33)–Mo(4)–Cl(40)	86.5(2)
Cl(13)–Mo(2)–CNT(2)	126.4(4)	Cl(33)–Mo(4)–CNT(4)	122.4(4)
Cl(20)–Mo(2)–CNT(2)	105.0(4)	Cl(40)–Mo(4)–CNT(4)	104.7(5)
Mo(1)–Cl(11)–Mo(2)	71.99(12)	Mo(3)–Cl(31)–Mo(4)	71.60(12)
Mo(1)–Cl(12)–Mo(2)	71.86(12)	Mo(3)–Cl(32)–Mo(4)	72.32(14)
Mo(1)–Cl(13)–Mo(2)	72.14(13)	Mo(3)–Cl(33)–Mo(4)	72.63(13)

[a] CNT(n) = centroid of atoms C(10n) through C(10n + 4).

only averages of chemically equivalent parameters over the two cations will be considered.

Each metal exhibits a four-legged piano stool geometry, the three bridging Cl and the terminal Cl ligand identifying the four legs for each metal. This geometry is ubiquitous to CpMo complexes, and has so far been observed for mononuclear complexes in the II (e.g. $[Cp^*Mo(CO)_3(PPh_3)]^+$ [14]), III (e.g. $Cp^*MoCl_2(PMe_3)_2$ [15]), IV (e.g. $Cp^*MoCl_3(PMe_3)$ [16]) and V (Cp^*MoBr_4) [17]) oxidation states, and for dinuclear Mo_2(I,I) (e.g. $Cp^*_2Mo_2(CO)_6$ [18]), Mo_2(III,III) (e.g. $(C_5H_4\text{-}i\text{-}Pr)_2Mo_2(\mu\text{-}Cl)_4$ [19]), Mo_2(III,IV) (e.g. $[Cp^*_2Mo_2(\mu\text{-}X)_4]^+$ (X = Br, I) [17]) and Mo_2(IV,IV) (e.g. $Cp^*_2Mo_2Cl_4(\mu\text{-}Cl)_2$ [9]) complexes. The structure of $[Cp^*_2Mo_2Cl_2(\mu\text{-}Cl)_3]^+$ is a rare example of two four-legged piano stools sharing *three* legs, another example being the Mo_2(III,III) complex $[Cp_2Mo_2(CO)_2(\mu\text{-}SMe)_3]^+$ [20].

The presence of a direct metal–metal bond is indicated not only by the Mo–Mo distance of 2.870(4) Å, but also by the diamagnetism as apparent from the ^1H NMR spectrum. The Mo–Mo distance, however, is significantly longer than those of all the other metal–metal bonded Mo(IV) dinuclear compounds that

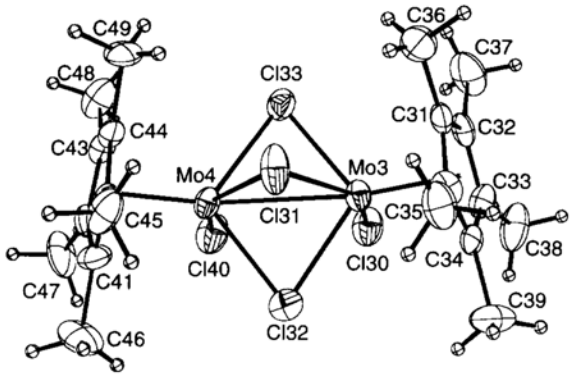

Fig. 1. An ORTEP view of the cation of compound $[Cp^*_2Mo_2Cl_5]^+[AlCl_4]^-$ with the numbering scheme employed. Ellipsoids are drawn at the 50% probability level. Hydrogen atoms are drawn with arbitrary radii.

we found in the literature (Mo–Mo bond length in parentheses): $[Mo(\mu\text{-}S)(SCNPr_2)(S_2CNPr_2)]_2$ (2.705(2) Å) [21], $Mo_2(O\text{-}i\text{-}Pr)_8$ (2.523(1) Å) [22], $[Mo(\mu\text{-}S)(SBu)_2(Me_2NH)]_2$ (2.730(1) Å) [23], $[Cl_3Mo(\mu\text{-}S_2)(\mu\text{-}Cl)_2MoCl_3]^{2-}$ (2.763(2) Å) [24], $Cp^*_2Mo_2(\mu\text{-}S)_2(\mu\text{-}S_2)$ (2.599(2) Å) [25] and a number of $[(ring)_2Mo_2(\mu\text{-}S)(\mu\text{-}SR)(\mu\text{-}S_2CH_2)]^+$ ions (ring = Cp, C_5H_4Me; R = Me, CH=CHPh, C(Ph)=CH_2) [26] (in the 2.599–2.610 Å range). Dinuclear non-bonded and paramagnetic Mo(IV) complexes also exist, however, e.g. $[Mo_2Cl_{10}]^{2-}$ [27]. The chemically most related molecule, namely the $Cp^*_2Mo_2Cl_6$ precursor, has structure **I** without a metal–metal bond (Mo···Mo = 3.888(1) Å) and it is paramagnetic [9]. On the other hand, the title compound is also geometrically related to the Mo(III) dimers $(ring)_2Mo_2Cl_4$ (structure **III**), where the Mo–Mo distance is 2.607(1) for ring = C_5H_4-i-Pr [19] and 2.598(2) Å (av.) for ring = C_5Me_4Et [28]. The $Cp^*_2Mo_2Cl_4$ compound was investigated electrochemically and shown to exhibit two successive one-electron oxidations but none of the oxidized products has been isolated [9]. As will be discussed later in relation to the MO calculations, the Mo–Mo bond is expected to be stronger in $(ring)_2Mo_2Cl_4$ than in $[(ring)_2Mo_2Cl_5]^+$, although the opposite would be predicted on the basis of a simple electron count.

It is useful to continue the comparison between the structure of the title compound (drawn again schematically in **IV**) and structure **III**; leaving aside for the moment considerations of oxidation state, structure **IV** can be ideally imagined as obtained from **III** by splitting a bridge by addition of an additional X atom. On going from **III** to **IV**, the variations of the CNT–Mo–Cl angles indicate the build-up of strain. In a mononuclear structure, these angles are generally around 110° for ligands such as Cl [29], whereas in a series of $(ring)_2Mo_2X_4$ and $[(ring)_2Mo_2X_4]^+$ compounds of structure **III** (X = Cl, Br, I), these angles are in the 119–121° range, irrespective of X [17]. On going to the $[Cp^*_2Mo_2Cl_5]^+$ structure, the two equatorial bridging chloride ligands (we define here the axis of the molecule as coinciding with the C_2 symmetry operator) increase their CNT–Mo–Cl angle to an average of 126(3)°, this increase being related to the increase in Mo–Mo distance and to the shorter Mo(IV)–$(\mu\text{-}Cl)_{eq}$ distance (2.433(6) Å) with respect to the Mo(III)–(μ-Cl) distance in **III** (av. 2.485(6) Å [19] for the C_4H_4-i-Pr and 2.488(3) Å [28] for the C_5Me_4Et compound). This is a stretching strain. On the other hand, the axial bridging Cl ligand shows CNT–Mo–Cl angles that average only 106.8(13)° and the average for the CNT–Mo–Cl angles to the terminal Cl ligands is even smaller, 104.8(13)°. This is a compression strain. The main cause for these effects and for the relatively long Mo–Mo distance is probably the repulsion between the two *syn* terminal Cl ligands, whose separation is only 3.22(4) Å (i.e. smaller than 3.60 Å, that is, twice the Cl van der Waal's radius).

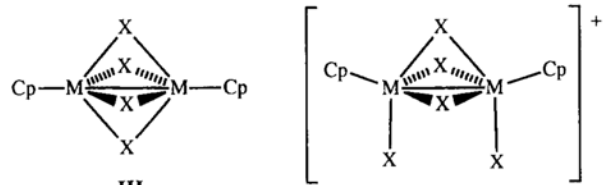

As may be expected, the terminal Mo–Cl bonds (average 2.358(11) Å) are shorter than the bridging ones. Among the latter, the bonds located equatorially (2.433(6) Å) are marginally shorter than those located axially (2.449(9) Å). No large difference in the Mo–Cl–Mo angles of equatorial versus axial ligands is observed, and the average value for the combined group (72.1(6)°) is substantially larger than the corresponding averages in compounds $(ring)_2Mo_2Cl_4$ (ring = C_5H_4-i-Pr, C_5Me_4Et) of type **III** (63.25(10) and 62.91(12)°, respectively) [19,28], this being another structural consequence of the larger Mo–Mo separation and shorter Mo–Cl bonds in the title compound. For the metal–metal *non-bonded* precursor $Cp^*_2Mo_2Cl_6$, these angles increase to 103.34(6)° [9]. The average Mo–CNT distance (2.02(2) Å) compares with that found in the $Cp^*_2Mo_2Cl_6$ precursor (2.028(7) Å) and the Cp* rings are slightly distorted from the η^5 configuration, the difference between shortest and longest Mo–C distances being 0.13(2), 0.12(2), 0.10(1) and 0.13(2) Å in the four rings, respectively.

3.3. Electronic structure

On the basis of simple electron counting rules, each metal in the $[Cp^*_2Mo_2Cl_5]^+$ ion has a 16-electron configuration if the metal–metal interaction is not considered. Given the NMR evidence for the diamagnetism of the complex, the formation of a metal–metal *double* bond could be predicted. However, the Mo–Mo bond

is found to be significantly longer in the title compound than in the quadruply-bridged systems $(ring)_2Mo_2Cl_4$ (type **III**), although in the latter one the metal–metal bond order is one. The Mo–Mo bond in $[Cp^*_2Mo_2Cl_5]^+$ is also longer relative to any of the dinuclear Mo(IV) compounds that do contain a bond [21–26]. These observations stimulated a more detailed MO analysis on the $[Cp_2Mo_2Cl_5]^+$ model complex, which we report here (see Fig. 2 for a summary of the salient results). Calculations on similar piano stool dimers, e.g. $Cp_2Mo_2(\mu\text{-}S)_2(\mu\text{-}S_2)$ and $Cp_2Mo_2(\mu\text{-}Cl)_4$, both of type **III**, have been reported before [30].

Qualitative considerations are very helpful to understand the nature of the electronic structure in this compound. The formation of the dinuclear core, electronically speaking, can be conveniently thought of as deriving from the combination of two mononuclear four-legged piano stool fragments, whose electronic structure is well known [31] and features two mostly metal-based orbitals in the frontier region, namely d_{z^2} and d_{xy}, the former one being at slightly higher energy (see Fig. 2, left-hand side). Upon combination of the two halves of the molecule in C_{2v} symmetry, the two d_{z^2} orbitals give rise to bonding and antibonding combinations of type a_1 and b_2, respectively, whereas the two d_{xy} orbitals give rise to combinations of type a_2 and b_1. If the two Mo–CNT vectors were perfectly co-linear such as in system **III**, these interactions could be ideally described as σ and δ and the diagram reported for $Cp_2Mo_2Cl_4$, which is qualitatively analogous to that obtained here, would result [30b]. On the other hand, these vectors form angles of $\sim 161°$ with the Mo–Mo vector and we feel justified to keep using the σ and δ labels for convenience. The σ and σ^* combinations are expected to differ substantially in energy because the two d_{z^2} orbitals have significant overlap, whereas the d_{xy} orbitals have a much poorer overlap giving rise to a much smaller separation between δ and δ^*. On the basis of d_{xy}–d_{xy} overlap only, the δ orbital (b_1) would be expected to be lower in energy than the δ^* orbital (a_2). However, the influence of the bridging Cl lone pairs can modify the picture in a way similar to what has been described before for other classes of compounds, e.g. the edge-sharing bioctahedral $M_2(\mu\text{-}X)_2L_8$ system [32] and system **III** [30b]. In both cases, the energy of the δ orbital is raised above that of the δ^* by the out-of-phase combination with the proper symmetry-adapted linear combination of the bridging ligands' lone pairs (in our case here, the p_x orbitals of the two equatorial ligands and the p_y orbital of the axial ligand). On the other hand, the δ^* orbital has no counterpart in the ligand orbitals with which to interact.

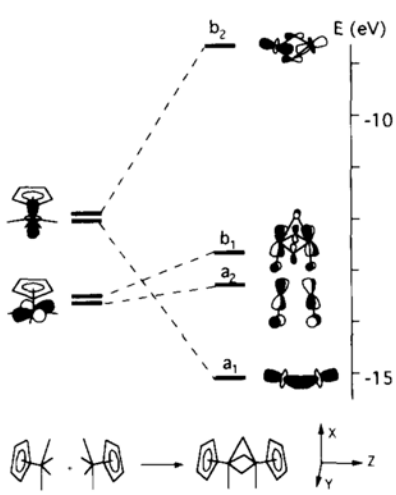

Fig. 2. An MO interaction diagram for the $[Cp_2Mo_2Cl_5]^+$ ion. The right hand side shows the energy and qualitative constitution of the MOs as they are calculated by the Fenske–Hall program. The master coordinate system used in the calculation is shown in the lower right hand side corner. The left hand side shows the energy and shape of the orbitals of the two ideal separated halves of the ion and are placed arbitrarily on the energy scale.

The results of the Fenske–Hall calculations are in perfect accord with all the above expectations (see Fig. 2, right-hand side). (For a listing of orbital energies for the relevant molecular orbitals and percent contributions of different types of atomic orbitals, see Section 5.) The b_1 orbital (LUMO, -12.30 eV) is raised in energy above the a_2 orbital (HOMO, -13.28 eV) by the antibonding interaction with the lone pairs of the bridging Cl atoms; the three bridging Cl atoms contribute about equally to this interaction (7.12% contribution from p_x orbitals of the two equatorial Cl atoms; 4.51% contribution from the p_y orbital of the axial Cl atom). An antibonding interaction exists, however, also with the two terminal Cl atoms' p_y orbitals (14.78%). The a_2 orbital has no contribution from the bridging Cl lone pairs and it has a greater contribution from the terminal Cl p_y orbitals with respect to the b_1 orbital (33.6%), but this is evidently not sufficient to keep the energy order as expected on the basis of the sole d_{xy}–d_{xy} overlap. The metal–metal σ-bonding orbital (a_1) is found at -15.16 eV, while the corresponding antibonding combination (b_2) is at -8.52 eV. The b_2 orbital has a significant contribution from the equatorial bridging Cl atoms' p_z lone pairs as illustrated in Fig. 2 (18.34%) whereas this contribution is absent (symmetry forbidden) in the a_1 orbital. There are, however, various other contributions of Cl lone pair combinations of proper symmetry type in the orbital a_1. The total contributions of metal atomic orbitals to the molecular orbitals illustrated in Fig. 2 are: 75.78% to a_1, 62.78% to a_2, 69.84% to b_1 and 74.04% to b_2.

The four available metal electrons occupy the MOs given in Fig. 2 to give rise to a $(a_1)^2(a_2)^2$, or $\sigma^2\delta^{*2}$ configuration; while the first orbital contributes sub-

stantially to the metal–metal attractive interaction ($d_{z^2} - d_{z^2}$ overlap population = 0.125), the latter provides a small destabilizing contribution (d_{xy}–d_{xy} overlap population = −0.050). The calculated HOMO–LUMO separation of 0.98 eV, although quantitatively not reliable, is qualitatively in accord with the diamagnetism of the ion (insignificant population of the excited $^3B_2$ state corresponding to the $(a_1)^2(a_2)^1(b_1)^1$ configuration).

We can address at this point the question: why is this Mo–Mo bond longer than the single bond in the Mo(III) dimers of type **III** (with X = Cl) or with respect to other Mo(IV)–Mo(IV) bonding distances? The MO diagram for system **III** [30b] is similar to the one derived here for system **IV**, with the additional pair of electrons occupying the δ orbital to give rise to a $\sigma^2\delta^{*2}\delta^2$ configuration. Literature data indicate that the Mo–Mo distance is substantially insensitive to the occupation of the δ orbital. For instance, the $[Cp^*_2Mo_2(\mu\text{-}Br)_4]^{n+}$ (n = 0,1) pair [17] shows identical Mo–Mo separations within experimental error and the distance in the Mo(IV) dimer $Cp^*_2Mo_2(\mu\text{-}S)_2(\mu\text{-}S_2)$, 2.599(2) Å [25] and in other Mo(IV) dimers of type **III**, e.g. $[(ring)_2Mo_2(\mu\text{-}S)(\mu\text{-}SR)(\mu\text{-}S_2CH_2)]^+$ (ring = η^5-C_5H_5, η^5-C_5H_4Me; 2.599–2.610 Å) [26] is not significantly different from those in tetrathiolato-bridged Mo(III) dimers, $(ring)_2Mo_2(\mu\text{-}SR)_4$ (2.596–2.603 Å) [33], and in the tetrachloro-bridged Mo(III) dimers mentioned above (Cl and S have approximately the same dimension). Only the size of the bridging donor atoms seems to affect the metal–metal separation: Mo–Mo distances for the series of tetrahalide compounds $(ring)_2Mo_2X_4$ are: 2.598(2) Å (X = Cl, ring = C_5Me_4Et) [28]; 2.643(4) (X = Br, ring = Cp*) [17]; 2.708(3) Å (X = I, ring = Cp*) [34]. For systems of type **III**, therefore, we can conclude that the Mo–Mo distance is substantially insensitive to the occupation of the δ orbital and depends mostly on the size of the bridging atoms. In short, the rigidity of the $M_2(\mu\text{-}X)_4$ moiety is restraining the metal–metal bond. The Mo(IV) $[Cp^*_2Mo_2Cl_4]^{2+}$ species is accessible electrochemically but it is too reactive to be isolated and structurally characterized. Theoretical predictions [30b] assign to it a $\sigma^2\delta^{*2}$ electronic configuration (namely identical to that of $[Cp_2Mo_2Cl_5]^+$) and, on the basis of the above arguments, its metal–metal separation should be close to that observed for the neutral Mo(III) compounds.

On going from **III** to structure **IV**, the structure partially opens up and the metal–metal bond gains flexibility. We can therefore argue that the destabilizing effect of the δ^* electrons can play a more important role here. In dinuclear systems containing multiple metal–metal bonds and no bridging ligands [1a], the occupation of δ orbitals has in general a limited effect which never amounts to as much as the difference of Mo–Mo separation between $[Cp_2Mo_2Cl_5]^+$ and $(ring)_2Mo_2Cl_4$ (ring = C_5H_4-i-Pr, C_5Me_4Et) systems, that is 0.27 Å. However, the metal–metal bonding in those systems is dominated by the stronger σ and π contributions, the δ bond being only a very small component of the overall metal–metal bonding, whereas in the Cp*Mo(IV) systems analyzed here, the bonding contribution is only provided by a 'bent' σ bond. The smaller σ bond overlap in **IV** with respect to **III** due to the bending of the bond can by itself be responsible for the weaker Mo–Mo interaction in the latter system. In addition, the higher Mo effective nuclear charge in the dinuclear Mo(IV) cation with respect to the dinuclear Mo(III) neutral complex is expected to contract the metal orbitals, resulting in a less effective overlap in the more oxidized complex. Finally, perhaps the most important factor could be the unfavorable *syn*-Cl–Cl interaction examined above within the context of the structural results. The calculations indeed confirm that this is a destabilizing interaction: the separation between in-phase and out-of-phase combinations of the terminal Cl p_z orbitals (**V** and **VI**, respectively) is large (1.94 eV, versus 1.19 and 0.09 eV between in- and out-of-phase combinations of the terminal Cl p_y and p_x orbitals, respectively), and the p–p orbital overlap populations reflect the repulsive interaction (−0.027, −0.010 and −0.001 for p_z, p_y and p_x orbitals, respectively). The molecular orbital corresponding to interaction **V** is in fact the highest energy lone-pair based MO and is located slightly above the Mo–Mo σ bonding orbital, at −15.03 eV.

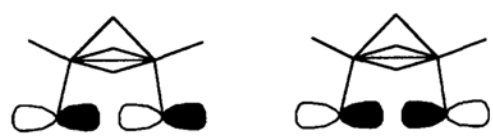

V VI

Other previously reported Mo(IV) dimers have different molecular and electronic structures (e.g. based on five-coordination geometries) that allow all the metal electrons to effectively participate in Mo–Mo bonding (e.g. compound $[Mo(\mu\text{-}S)(SBu)_2(Me_2NH)]_2$ has a double ($\sigma^2\pi^2$) metal–metal bond [23]) and/or smaller bridging donor atoms (e.g. oxygen in $Mo_2(O\text{-}i\text{-}Pr)_2$ [22] and/or weaker interligand repulsions. Presumably for one or more of these reasons, the Mo–Mo bond distance in $[Cp^*_2Mo_2Cl_5]^+$ is longer than for any of these previously reported compounds.

3.4. Reaction with Cl^-. Structure I versus II for $Cp^*_2Mo_2Cl_6$

$[Cp^*_2Mo_2Cl_5]^+[AlCl_4]^-$ reacts instantaneously with an excess of Cl^- in CH_2Cl_2 at room temperature to give the $[Cp^*MoCl_4]^-$ ion. This reaction presumably occurs in two stages, the first one being the addition of a Cl^- ion to afford the neutral hexachloro parent

dimer (Eq. (3)). Then, the latter compound reacts with additional Cl^- to form the anion (Eq. (4)), as has been reported before [9].

$$[Cp^*_2Mo_2Cl_5]^+ + Cl^- \longrightarrow Cp^*_2Mo_2Cl_6 \quad (3)$$

$$Cp^*_2Mo_2Cl_6 + 2Cl^- \longrightarrow 2[Cp^*MoCl_4]^- \quad (4)$$

The dinuclear intermediate is not observed spectroscopically when an excess of Cl^- is added. However, when CD_2Cl_2 solutions of the tetrachloroaluminate salt *without* any added chloride salt are investigated by ^1H NMR, a minor amount of $Cp^*_2Mo_2Cl_6$ is always observed. This material may already be present as an impurity in the salt, but it could also be formed again from the dinuclear cation because of the release of Cl^- from the anion by the establishment of equilibria with oligonuclear aluminate ions (e.g., Eq. (5)). In other words, the $[Cp^*_2Mo_2Cl_5]^+$ ion may be sufficiently Lewis acidic to compete with $AlCl_3$ for Cl^- (Eq. (6)). Equilibrium (5) has been investigated in melts [35], and the structural characterization of several $[Al_2Cl_7]^-$ salts obtained by solution methods has been reported, for instance $[(C_6Me_6)_3Zr_3Cl_6][Al_2Cl_7]_2$ [36]. Yet another possibility is that Cl^- is released from $[AlCl_4]^-$ by the interaction with adventitious donors S, e.g. water, see Eq. (7).

$$2[AlCl_4]^- \rightleftharpoons [Al_2Cl_7]^- + Cl^- \quad (5)$$

$$[Cp^*_2Mo_2Cl_5]^+ + 2[AlCl_4]^- \rightleftharpoons [Al_2Cl_7]^- + Cp^*_2Mo_2Cl_6 \quad (6)$$

$$[AlCl_4]^- + S \rightleftharpoons AlCl_3(S) + Cl^- \quad (7)$$

Whatever the source of the neutral dimer, one consideration that comes immediately to mind is that attack of the cation by Cl^- should lead naturally to the *syn* structure **II** rather than to the observed structure **I** for the dinuclear product of Eq. (3). A $Cp^*_2Mo_2Cl_6$ isomer with structure **II** could be metal–metal bonded and diamagnetic (the MO scheme is expected to be similar to that presented here for the $[Cp_2Mo_2Cl_5]^+$ cation). On the other hand, no new product forms upon dissolution of the tetrachloroaluminate salt, only the paramagnetic isomer with structure **I** does. The important implication of this observation is that a hypothetical $Cp^*_2Mo_2Cl_6$ dimer of type **II**, if formed, isomerizes quickly to the alternative, paramagnetic structure **I**. On the basis of the results of the calculations illustrated above, we have learned that the opening of one bridge from structure **III** to structure **IV** weakens substantially the Mo–Mo interaction for a number of reasons, one of them being the introduction of ligand–ligand repulsions. Therefore, we extrapolate that the opening of one additional bridge on going from structure **IV** of $[Cp^*_2Mo_2Cl_5]^+$ to a hypothetical structure **II** for $Cp^*_2Mo_2Cl_6$ will weaken further the Mo–Mo interaction to the point of inducing the conversion to the isomeric structure **I**.

3.5. Electrochemical behavior

We had implicated before a neutral $Cp^*_2Mo_2Cl_5$ species in the mechanism of formation of $Cp^*_2Mo_2Cl_6$ [9] and had proposed for it a structure identical with the one that we have now found for the $[Cp^*_2Mo_2Cl_5]^+$ cation. Therefore, we were expecting to observe a reversible reduction process for the title compound. Indeed, the compound shows a reversible reduction at $E_{1/2} = -0.13$ V in CH_2Cl_2 solution. This wave comes suspiciously close to the reversible wave that we reported for the $[Cp^*MoCl_4]^-/Cp^*MoCl_4$ couple ($E_{1/2} = -0.16$ V) [9], but the absence of such species from solution is firmly established by the ^1H NMR study and by the observation that the cyclic voltammogram remains unaltered after the addition of a large excess of $AlCl_3$. The observation of a diffusion limited anodic current while holding the potential at $E > -0.13$ V is consistent with the presence of $Cp^*_2Mo_2Cl_5$ impurities in the sample, in agreement with the spectroscopic characterization of the material (see Section 2). At $E < -0.13$ V, a diffusion limited cathodic current is observed. Past the first reduction process, other ill-defined reductive processes are observed, but no indication of reversibility is evident at scan rates up to 500 mV s^{-1}. Thus, after reduction to $[Cp^*_2Mo_2Cl_5]^-$, a rearrangement to a different structural type or further chemical reactivity must rapidly take place. We would like to point out that the reducing electrons occupy the b_1 orbital in Fig. 2, which has a significant Mo–(μ-Cl) π^* component, therefore the reduction process is expected to weaken the Mo–(μ-Cl) bonds and perhaps cause an opening of the bridge system. In this respect, it is relevant to note that the related complex $[Cp_2Mo_2Cl_5]^-$, i.e. the Cp analogue of the product of two-electron reduction of the title compound, has a completely different structure with a single Cl bridge and an Mo–Mo triple bond, see **VII** [37].

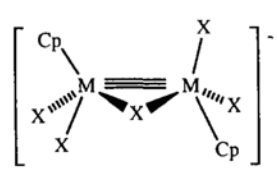

VII

4. Conclusions

The $[Cp^*_2Mo_2Cl_5]^+$ ion has a novel structural type for Cp*Mo(IV) halide complexes. We have reported here its molecular and electronic structure, and examined in detail the metal–metal bonding interaction. A greater number of bridging chloride ligands (or more

specifically a smaller number of terminal Cl ligands) favors a short contact between the two metal centers, whereas the addition of terminal Cl^- ligands weakens the Mo–Mo interaction. In this respect, $[Cp^*_2Mo_2Cl_5]^+$ finds its proper place between $[Cp^*_2Mo_2Cl_4]^{n+}$ ($n = 0$, 1, 2) and the non-bonded $Cp^*_2Mo_2Cl_6$.

5. Supplementary material

Full tables of crystal data, bond distances and angles, anisotropic displacement parameters and hydrogen atom coordinates (20 pages), and a listing of molecular orbitals and % contribution from atomic orbital for the model system $[Cp_2Mo_2Cl_5]^+$ (1 page) are available from the authors on request. The crystallographic tables have also been deposited with the Cambridge Crystallographic Data Centre.

Acknowledgements

We are grateful to the DOE-OER for support of this work under contract DE-FG05-92ER 14230. Additional support from the NSF and the Alfred P. Sloan Foundation through awards to R.P. is also gratefully acknowledged.

References

[1] (a) F.A. Cotton and R.A. Walton, *Multiple Bonds Between Metal Atoms,* Wiley, New York, 1982; (b) S. Shaik, R. Hoffmann, C.R. Fisel and R. Summerville, *J. Am. Chem. Soc., 102* (1980) 4555; (c) J.J.H. Edema and S. Gambarotta, *Comments Inorg. Chem., 11* (1991) 195.

[2] A.R. Chackravarty, F.A. Cotton, M.P. Diebold, D.B. Lewis and W. Roth, *J. Am. Chem. Soc., 108* (1986) 971.

[3] J.A. Jaecker, W.R. Robinson and R.A. Walton, *J. Chem. Soc., Dalton Trans.,* (1975) 698.

[4] F.A. Cotton, M. Matusz and R.C. Torralba, *Inorg. Chem., 30* (1991) 4392.

[5] (a) R. Poli and H.D. Mui, *Inorg. Chem., 30* (1991) 65; (b) H.D. Mui and R. Poli, *Inorg. Chem., 28* (1989) 3609.

[6] R. Poli and J.C. Gordon, *J. Am. Chem. Soc., 114* (1992) 6723.

[7] J.D. Bryan, D.R. Wheeler, D.L. Clark, J.C. Huffman and A.P. Sattelberger, *J. Am. Chem. Soc., 113* (1991) 3184.

[8] U. Kölle, J. Kossakowski, N. Klaff, L. Wesemann, U. Englert and G.E. Herberich, *Angew. Chem., Int. Ed. Engl, 30* (1991) 690.

[9] F. Abugideiri, G.A. Brewer, J.U. Desai, J.C. Gordon and R. Poli, *Inorg. Chem., 33* (1994) 3745.

[10] C. Ting and L. Messerle, *Inorg. Chem., 28* (1989) 173.

[11] W.A. Herrmann, R.A. Fischer, J.K. Felixberger, R.A. Paciello, P. Kiprof and E. Herdtweck, *Z. Naturforsch., Teil B, 43* (1988) 1391.

[12] (a) A.C.T. North, D.C. Phillips and F.S. Mathews, *Acta Crystallogr., Sect. A, 24* (1968) 351; (b) E.J. Gabe, Y. Le Page, J.P. Charland, F.L. Lee and P.S. White, *J. Appl. Crystallogr., 22* (1989) 384; (c) G. Sheldrick, *SHELXS,* University of Göttingen, Germany, 1986.

[13] (a) M.B. Hall and R.F. Fenske, *Inorg. Chem., 11* (1972) 768; (b) M.B. Hall, *Fenske–Hall Program,* Version 5.1, a program for the Macintosh, Texas A&M, College Station, TX, 1990.

[14] P. Leoni, E. Aquilini, M. Pasquali, F. Marchetti and M. Sabat, *J. Chem. Soc., Dalton Trans.,* (1988) 329.

[15] R.T. Baker, J.C. Calabrese, R.L. Harlow and I.D. Williams, *Organometallics, 12* (1993) 163.

[16] F. Abugideiri, J.C. Gordon, R. Poli, B.E. Owens-Waltermire and A.L. Rheingold, *Organometallics, 12* (1993) 1575.

[17] (a) J.U. Desai, J.C. Gordon, H.-B. Kraatz, B.E. Owens-Waltermire, R. Poli and A.L. Rheingold, *Angew. Chem., Int. Ed. Engl., 32* (1993) 1486; (b) J.U. Desai, J.C. Gordon, H.-B. Kraatz, V.T. Lee, B.E. Owens-Waltermire, R. Poli, A.L. Rheingold and C.B. White, *Inorg. Chem., 33* (1994) 3752.

[18] P. Leoni, F. Marchetti, M. Pasquali and P. Zanello, *J. Chem. Soc., Dalton Trans.,* (1988) 635.

[19] P.D. Grebenik, M.L.H. Green, A. Izquierdo, V.S.B. Mtetwa and K. Prout, *J. Chem. Soc., Dalton Trans.,* (1987) 9.

[20] M.B. Gomes de Lima, J.E. Guerchais, R. Mercier and F. Pétillon, *Organometallics, 5* (1986) 1952.

[21] (a) L. Ricard, J. Estienne and R. Weiss, *J. Chem. Soc., Chem. Commun.,* (1972) 906; (b) *Inorg. Chem., 12* (1973) 2182.

[22] M.H. Chisholm, F.A. Cotton, M.E. Extine and W.W. Reichert, *Inorg. Chem., 17* (1978) 2944.

[23] M.H. Chisholm, J.F. Corning and J.C. Huffman, *Inorg. Chem., 21* (1982) 286.

[24] U. Müller, P. Klingelhöfer, C. Friebel and J. Pebler, *Angew. Chem., Int. Ed. Engl., 24* (1985) 689.

[25] H. Brunner, W. Meier, J. Wachter, E. Guggolz, T. Zahn and M.L. Ziegler, *Organometallics, 1* (1982) 1107.

[26] (a) C.J. Casewit, R.C. Haltiwanger, J. Noordik and M. Rakowski Dubois, *Organometallics, 4* (1985) 119; (b) J.C.V. Laurie, L. Duncan, R.C. Haltiwanger, R.T. Weberg and M. Rakowski Dubois, *J. Am. Chem. Soc., 108* (1986) 6234; (c) R.T. Weberg, R.C. Haltiwanger, J.C.V. Laurie and M. Rakowski Dubois, *J. Am. Chem. Soc., 108* (1986) 6242.

[27] E. Hey, F. Weller and K. Dehnicke, *Z. Anorg. Allg. Chem., 508* (1984) 86.

[28] K. Fromm and E. Hey-Hawkins, *Z. Anorg. Allg. Chem., 619* (1993) 261.

[29] R. Poli, *Organometallics, 9* (1990) 1892.

[30] (a) B.E. Bursten and R.H. Cayton, *Inorg. Chem., 28* (1989) 2846; (b) J.C. Green, M.L.H. Green, P. Mountford and M.J. Parkington, *J. Chem. Soc., Dalton Trans.,* (1990) 3407.

[31] (a) P. Kubacek, R. Hoffmann and Z. Havlas, *Organometallics, 1* (1982) 180; (b) H. Schmidt and D. Rehder, *Transition Met. Chem. (Weinheim), 5* (1980) 214.

[32] (a) S. Shaik, R. Hoffmann, C.R. Fisel and R.H. Summerville, *J. Am. Chem. Soc., 102* (1980) 4555; (b) L.B. Anderson, F.A. Cotton, D. De Marco, A. Fang, W.H. Ilsley, B.W.S. Kolthammer and R.A. Walton, *J. Am. Chem. Soc., 103* (1981) 5078; (c) F.A. Cotton, M.P. Diebold, C.J. O'Connor and G.L. Powell, *J. Am. Chem. Soc., 107* (1985) 7438; (d) A.R. Chakravarty, F.A. Cotton, M.P. Diebold, D.B. Lewis and W.J. Roth, *J. Am. Chem. Soc., 108* (1986) 971; (e) R. Poli and H.D. Mui, *Inorg. Chem., 30* (1991) 65; (f) R. Poli and R.C. Torralba, *Inorg. Chim. Acta, 212* (1993) 123.

[33] (a) N.G. Connelly and L.F. Dahl, *J. Am. Chem. Soc., 92* (1970) 7470; (b) M. McKenna, L.L. Wright, D.J. Miller, L. Tanner, R.C. Haltiwanger and M. Rakowski Dubois, *J. Am. Chem. Soc., 105* (1983) 5329.

[34] J.H. Shin and G. Parkin, *Polyhedron, 13* (1994) 1489.

[35] M. Lipsztajn and R.A. Osteryoung, *Inorg. Chem., 23* (1984) 164, and refs. therein.

[36] F. Stollmaier and U. Thewalt, *J. Organomet. Chem., 208* (1981) 327.

[37] R. Poli and A.L. Rheingold, *J. Chem. Soc., Chem. Commun.,* (1990) 552.